Mineralogy and Petrology

Carbon and nitrogen systematics in nitrogen-rich ultradeep diamonds from San Luiz, Brazil

--Manuscript Draft--

Manuscript Number:		
Full Title:	Carbon and nitrogen systematics in nitrogen-rich ultradeep diamonds from San Luiz, Brazil	
Article Type:	Supplement Kimberlites	
Keywords:	Transition zone Lower mantle Carbon Isotopes Nitrogen isotopes Solid molecular nitrogen δ-N2	
Corresponding Author:	Oded Navon Hebrew University of Jerusalem Gerusalem, ISRAEL	
Corresponding Author Secondary Information:		
Corresponding Author's Institution:	Hebrew University of Jerusalem	
Corresponding Author's Secondary Institution:		
First Author:	Oded Navon	
First Author Secondary Information:		
Order of Authors:	Oded Navon	
	Thomas Stachel	
	Richard Stern	
	Jeffrey W Harris	
Order of Authors Secondary Information:		
Funding Information:	German-Israeli Foundation for Scientific Research and Development (I-1239-301.8/2014)	Prof. Oded Navon
	NSERC Discovery Grant	Prof. Thomas Stachel

Carbon and nitrogen systematics in nitrogen-rich, ultradeep diamonds from Sao Luiz, Brazil

O. Navon[1] • T. Stachel[2]• R. A. Stern[2] • J. W. Harris[3]

✉ O. Navon

Oded.Navon@mail.huji.ac.il

[1] Institute of Earth Sciences, The Hebrew University of Jerusalem, Israel, 9190401

[2] Canadian Centre for Isotopic Microanalysis, Department of Earth and Atmospheric Sciences, University of Alberta, Edmonton, AB, Canada T6G 2E3

[3] School of Geographical and Earth Sciences, The Gregory Building, Lilybank Gardens, Glasgow, G12 8QQ, UK

Abstract Three diamonds from Sao Luiz, Brazil carrying nano- and micro-inclusions of molecular δ-N_2 that exsolved at the base of the transition zone were studied for their carbon and nitrogen isotopic composition and the concentration of nitrogen utilizing SIMS. The diamonds are individually uniform in their carbon isotopic composition and most spot analyses yield $\delta^{13}C$ values of -3.2±0.1‰ (ON-SLZ-390) and -4.7±0.1‰ (ON-SLZ-391 and 392). Only a few analyses deviate from these tight ranges and all fall within the main mantle range of -5±3‰. Most of the nitrogen isotope analyses also have typical mantle $\delta^{15}N$ values (-6.6±0.4‰, -3.6±0.5‰ and -4.1±0.6‰ for ON-SLZ-390, 391 and 392, respectively) and are associated with high nitrogen concentrations of 800-1250 atomic ppm. However, some nitrogen isotopic ratios, associated with low nitrogen concentrations (<400 ppm) and narrow

zones with bright luminescence are distinctly above the average, reaching positive $\delta^{15}N$ values. These sharp fluctuations can neither be attributed to fractionation nor are they easily explained by introduction of new pulses of melt or fluid. We discuss the possibility that they result from fractionation between different growth directions, so that distinct $\delta^{15}N$ values and nitrogen concentrations may form during diamond growth from a single melt/fluid. Other more continuous variations, in the core of ON-SLZ-390 or the rim of ON-SLZ-392 may be the result of Rayleigh fractionation or mixing.

Key words:

Transition zone

Lower mantle

Carbon Isotopes

Nitrogen isotopes

Solid molecular nitrogen

δ-N_2

Character count: 39,983 Characters (with spaces)

33,746 Characters (no spaces)

Introduction

Diamonds from the lower mantle and the transition zone (superdeep diamonds) have been known for more than 30 years (Scott-Smith et al. 1984; Moore and Gurney 1985) and have turned into a major source of information of these otherwise inaccessible parts of the Earth. While most attention has been given to the composition of mineral inclusions in these rare samples, the diamonds themselves also carry interesting information in their carbon isotopic composition and in the concentration, isotopic composition and speciation of nitrogen and other impurities in the diamond matrix. Additional information is stored in the nature and spatial distribution of other color and fluorescence centers, but except for using fluorescence or cathodoluminescence (CL) as a guide for diamond growth history (as we do here), we do not yet know how to read the geological information that may be stored in the variation of the CL intensity.

Many superdeep diamonds carry almost no nitrogen (Type II diamonds). Where present, nitrogen is commonly less than 200 ppm and is highly aggregated, with most or all nitrogen in B centers (four nitrogen atoms surrounding a vacancy) or associated with hydrogen in VN3H centers (three nitrogen atoms surrounding a vacancy decorated by a hydrogen atom). The rates of conversion of nitrogen from single substitutional (C centers) to couplets (two nitrogen atoms replacing two carbon atoms, A centers) and to B centers depends on the concentration of nitrogen, [N], and on the temperature. The present calibration of the kinetics of the A to B conversion dictates a geologically fast conversion of most nitrogen to B centers at transition zone or lower mantle temperatures. For example, at 1500°C, 99.9% of the A centers of a diamond with 100 ppm nitrogen would convert to B centers in just ~0.1 Gy (Taylor et al. 1990, 1996). Still, some superdeep diamonds are reported to have A centers and low B/(B+A) ratios (Davies et al. 2004a).

The $\delta^{13}C$ values of most diamonds that carry lower mantle inclusions average -4.5±2.6‰ (1σ), overlapping the predominant mantle value of -5‰ (Javoy et al. 1986). However, more negative values were also reported (Bulanova et al. 2010). Most of the inclusions are of "peridotitic" affinity (many ferropericlase inclusions and some bridgmanites). Those carrying minerals typical of the transition zone (mostly majoritic garnets of eclogitic or, rarely, peridotitic affinity) span a much wider range: -8.4±7.1‰. The majority are close to the mantle range, but quite a few exhibit more negative values down to -25‰.

Compared with over 200 analyses of carbon isotopic composition, nitrogen isotopic composition was measured in only ~50 ultradeep samples, reflecting the very low nitrogen concentrations in many superdeep diamonds. Most are lower mantle diamonds and only a few are of possible transition zone origin. Most lower mantle diamonds have $\delta^{15}N$ of -1 to -5‰, but a few span a wider range between +5 and -10‰ (average -3.4±4.4‰). The few $\delta^{15}N$ values for transition zone diamonds span a much wider range (-40 to +10‰) with most values at -10 to +10‰ (Palot et al. 2012, 2017).

The three diamonds we studied are unique in their very high nitrogen content and in the way in which their depth of origin was determined. Navon et al. (2017) detected 100% of B centers and only negligible contribution from platelets that were probably degraded, making them highly irregular diamonds (Woods 1986). Transmission electron microcopy (TEM) revealed the presence of nanometric inclusions of bimodal size distribution (~200 nm and ~20 nm). Navon et al. (2017) used Raman spectroscopy to identify the content of these inclusions as δ-N_2, a high-pressure polymorph of molecular nitrogen, and calculated an internal pressure of 10.9±0.5 GPa based on the shift of the Raman lines. Using the phase diagram and the equations of state of fluid N_2 and diamond, they estimated the internal pressure at mantle temperatures (along a geotherm) and suggested that the inclusions were formed at ~22 GPa, corresponding to depth of more than 600 km and temperatures of more than 1600°C, at the base of the transition zone. They suggested that the nanometric inclusions were formed by

exsolution of nitrogen that resided in platelets and B centers as the diamond descended into the base of the transition zone in a down-going convecting mantle current. Navon et al. (2017) estimated that the diamonds carry ~900 ppm nitrogen in B centers and an additional 500 ppm of δ-N_2 in the zones populated by the exsolutions.

Similar diamonds have been studied before by physicists who characterized the nanoinclusions, which were designated "voidites" (e.g., Bruley and Brown 1989; Luyten et al. 1994; Kiflawi and Bruley 2000). However, they did not reach a definite identification of the trapped phase. They were also studied by geologists (Kaminsky et al. 2001, 2015; Rudloff-Grund et al. 2016; Kagi et al. 2016), but again, with no clear determination of their content or origin.

The high nitrogen content and the good spatial resolution of secondary ion mass spectrometry (SIMS) combined with detailed CL imaging of the diamonds allow us to examine in detail the systematics of both carbon and nitrogen isotopes as well as the variations in the concentration of nitrogen and in the CL intensity and to compare them to previous studies of other superdeep diamonds.

Samples

The three samples we studied are a subset of the diamonds described and studied by Navon et al. (2017) and were described there. They are a few mm in size (Fig. 1) and weigh 69–126 mg. All were laser-cut in a random crystallographic orientation by a commercial diamond cutter and polished on a diamond wheel to produce 0.8–1.1mm thick slabs with parallel surfaces. Examination of the slabs under an optical microscope yielded no mineral inclusions.

They are translucent due to the presence of clouds of inclusions that are barely seen, even at the highest magnification.

Methods

Sample preparation

The polished slabs were cleaned ultrasonically in a mixture of 69% HNO_3 and 60% HF and rinsed in water and ethanol. They were cast into a small epoxy block which was pressed into indium along with the CCIM reference materials, diamond S0270 and vitreous carbon S0233A and the mount (M1430) was coated with 5 nm of gold.

Cathodoluminescence (CL)

CL images were obtained using a a Zeiss EVO MA15 scanning electron microscope (SEM) equipped with a parabolic mirror coupled to a high-sensitivity, broadband photomultiplier detector. The SEM was operated at 15 kV and 3 – 5 nA beam current. Along with the CL images, we also collected secondary electron images of the diamonds. Following the CL imaging, the mount was coated with an additional 35 nm gold film prior to SIMS analysis

SIMS

Carbon isotopes ($^{13}C/^{12}C$), N abundances, and N-isotopes ($^{15}N/^{14}N$) were determined in separate sessions using the CCIM IMS-1280 multi-collector ion microprobe using methods and reference materials detailed by Stern et al. (2014) with slight modifications as noted here. Primary beam conditions included the use of 20 keV $^{133}Cs^+$ ions focused to a beam diameter

of ~12 µm, and beam currents of 1.0 – 2.5 nA. The primary beam was rastered across a 20 x 20 µm area prior to analysis to clean the surface of Au and contaminants and to implant Cs. C-isotopes were analyzed first, with subsequent N-abundance and N-isotope measurements done directly from the identical spot location.

Negative secondary ions were extracted through 10 kV to the grounded secondary column (Transfer section). Automated tuning of the secondary ions in the Transfer section preceded each analysis. Secondary ion collection conditions for C-isotopes included an entrance slit width of 110 µm, field aperture of 5 x 5 mm, a field aperture-to-sample magnification of 100x, and a fully-open energy slit. Both $^{12}C^-$ and $^{13}C^-$ were analyzed simultaneously in Faraday cups (L'2 using 10^{10} Ω amplifier circuit, and FC2 with 10^{11} Ω) at mass resolutions of 2000 and 2900, respectively. Mean count rates for $^{12}C^-$ and $^{13}C^-$ were typically 1.0×10^9 and 1.0×10^7 counts/s, respectively, determined over a 75 s counting interval. Total spot-to-spot analysis time (including pre-analysis raster, automated secondary ion tuning, and peak counting) for each measurement was 210 s.

For N-abundances, secondary ion collection conditions utilized a magnification of 133x, an entrance slit width of 45 µm, field aperture of 3×3 mm, and energy slit width of 40 eV transmitting low-energy ions. The molecular ions [$^{12}C^{13}C^-$] and [$^{13}C^{14}N^-$] were measured simultaneously using a Faraday cup – electron multiplier combination (L'2 using 10^{11} Ω amplifier, and EM axial detector, respectively) at mass resolutions of 6000 and 5500, respectively, sufficient to resolve any potential spectral interferences. Electron multiplier counts were corrected for background and deadtime (40 ns).

Nitrogen isotopes ($^{15}N/^{14}N$) were determined last with secondary ion collection conditions identical to that for N-abundances. The $^{12}C^{14}N^-$ and $^{12}C^{15}N^-$ molecular ions were analyzed simultaneously in a Faraday cup – EM combination at mass resolutions of >6200 (offset peak center position) and 5500, respectively. Mean count rates for which N-isotope data are reported ranged from 1.1×10^6 – 2.1×10^7 counts/s for $^{12}C^{14}N^-$, and from 4.5×10^3 –

8.0×10^4 counts/s for $^{12}C^{15}N^-$, determined over a 300 s counting interval. A Faraday cup baseline for N-isotopes was measured prior to each analysis. Electron multiplier counts were corrected for background and deadtime. Total spot-to-spot analysis time was 480 s.

The analytical sequence for C-isotopes interspersed measurements of unknowns with the diamond RM S0270 having a $\delta^{13}C_{VPDB}$ = -8.88 ±0.10‰ in a 4:1 ratio. Instrumental mass fractionation (IMF) for $^{13}C^-/^{12}C^-$ was determined from utilizing all the replicate analyses of S0270 for one session (N = 40), where the standard deviation of the $^{13}C^-/^{12}C^-$ values was 0.05 ‰, after correction for systematic within-session IMF drift of 0.1 ‰ over several hours. Uncertainties of individual $\delta^{13}C_{VPDB}$ analyses propagate within-spot (~0.05‰, 1σ), between-spot (0.05‰, 1σ, blanket assigned), and between-session errors (0.01‰, 1σ), and are typically ±0.14 ‰ (2σ). The spot uncertainties exclude the error in the value of the RM reported above, which can be added as appropriate for comparisons with other data, but which would otherwise mask real differences between the diamonds analyzed.

For N-abundances, the $[^{13}C^{14}N]^-/[^{12}C^{13}C]^-$ ratios in unknowns and S0270 diamond were analyzed in the same sequence as for C-isotopes. The sensitivity factor for $[^{13}C^{14}N]^-/[^{12}C^{13}C]^-$ was determined from S0270 diamond whose N-abundance was calibrated relative to S0280E diamond having a N abundance of 1670 at. ppm (±5‰ absolute, 2σ) located on a separate mount. The uncertainties in the N abundance measurements reported include within-spot, between-spot, and between-session errors.

The analytical sequence for N-isotopes interspersed measurements of unknowns with pieces of diamond S0270, having $\delta^{15}N_{AIR}$ = -0.40 ± 0.50‰ in a 4:1 ratio. IMF was determined during one analytical session from utilizing all the replicate $^{12}C^{15}N^-/^{12}C^{14}N^-$ analyses of S0270, for which the standard deviation was ±0.15‰ after correction for minor (-0.3 ‰) within-session IMF drift. Uncertainties of individual $\delta^{15}N$ analyses propagate within-spot counting errors and between-session errors (±0.05 ‰, 1σ). The 95% confidence uncertainty for $\delta^{15}N_{AIR}$ averaged ±0.48‰ for individual analyses of S0270, and for the

unknowns with variable N concentration ranged from ±0.6 – 1.5‰. The spot uncertainties exclude the error in the value of the RM reported above, which can be added as appropriate for comparisons with other data. Nitrogen abundances were also calculated from the N-isotope data using primary-beam-normalized secondary ion yields of $^{12}C^{14}N^-$ normalized to the mean yield for diamond S0270.

Results

CL and diamond growth

The CL images of the three diamonds are presented in Fig. 1 and Table 1 and reveal complex patterns. The patterns represent varying conditions during growth, but are also affected by the exposure of 3-dimensional structures on 2-dimensional surfaces formed by the cutting and polishing of the samples.

ON-SLZ-390: The core reveals low luminescence and straight octahedral surfaces (zone a, analysis spots 1-3). It is surrounded by a dark zone (b, 4) and both zones (a and b) are strongly resorbed, leaving an elongated diamond with smooth faces. This diamond was overgrown by an oscillatory zone with bright CL response (c, 5) and then by more uniform growth of larger octahedral planes (d, 6-7), which turned into a uniform zone with intermediate brightness in CL (e, 8-15). In one corner, further resorption and growth of diamond of darker luminescence is exposed (f, not analyzed).

ON-SLZ-391: The CL displays a complex pattern of alternating brighter and darker straight zones that are generally concentric, but outline two separate centers of growth. The SIMS profile extends from one center (a) to the rim (f) and samples the entire exposed growth history. The central part (a, 1-5) ends with a dissolution event followed by growth of a darker

layer (b, 6), a bright discontinuous layer (c, 7) and a thick outer growth zone (d and f, 8-13) interrupted by one thin bright layer (e, 12).

ON-SLZ-392: The diamond is a broken piece from a larger crystal, but it includes the center of growth (a, 1-3) that ends with a brighter zone that was resorbed on one side. Growth continued with straight octahedral faces of darker CL (b, 4-6) followed by a few very bright narrow bands (c, 7) that are also exposed in the triangular area further out along the profile (b1, c spots 9, 10). Further growth is initially associated with intermediate CL response (d, 11-12) that becomes brighter towards the rim (e and f, 8, 13-14). The triangular exposure is the result of a bulge that grew from the main octahedron and is now cut by the polished surface, exposing the older parts of the d layer, then the bright c layer and finally the older b layer at the center of the buldge.

$\delta^{13}C$, $\delta^{15}N$ and [N]

ON-SLZ-390: The CL reveals two parts that are separated by a dissolution event. The carbon isotopes clearly follow this division. In the core of this diamond (zones a and b in Fig. 1) carbon trends from -3.1 to -2.4‰ (Fig. 2). Passing the dissolution boundary, $\delta^{13}C$ falls to -3.26‰ and remains constant all the way to the rim with less than 0.1‰ deviation from an average value of -3.23‰. The inner parts (a and b) have < 5 ppm nitrogen. The surrounding growth layers (c and d) have low nitrogen (~200 ppm) with $\delta^{15}N$ values of -0.2 and +0.9‰. Then, over a minor boundary in the CL (from zone d to zone e) and uniform carbon isotopic composition, both [N] and $\delta^{15}N$ change abruptly. The $\delta^{15}N$ drops from around 0 down to -6.1‰, followed by a minor decrease to -7.0‰ at the rim. The concentration of nitrogen changes from ~200 to ~1000 ppm across the boundary from zone d to e, and then remains constant within a narrow range of 1020±50 ppm. In summary, the diamond reveals

decoupling between carbon and nitrogen and correlative behavior of the concentration and the isotopic composition of nitrogen.

ON-SLZ-391: The inner zone (a, 1-5) is uniform in its isotopic values and nitrogen, except in one spot (4) where CL is bright and [N] is somewhat lower. A minor dissolution event between zone a and zone b has no effect on the carbon isotopic composition, the nitrogen isotopic ratio slightly decreases, but nitrogen concentration rises from 830±100 in zone a to 1080±80 in the outer zones. Overall, the $\delta^{13}C$ values are homogeneous across the diamond at -4.75±0.08‰ (1σ) and $\delta^{15}N$ is also fairly uniform (-3.6±0.5‰), except in two narrow bright layers (c and e) where $\delta^{15}N$ values are higher at -1.06 and +0.45‰ and [N] falls from 1080 to 340 ppm. In summary, in spite of the oscillatory CL response, the isotopic ratios are uniform except for two 50-100 μm thick layers with bright CL, higher $\delta^{15}N$ and lower [N].

ON-SLZ-392: Like ON-SLZ-391, this diamond is also characterized by uniform carbon isotopic ratios throughout the diamond ($\delta^{13}C$ of -4.7±0.1‰), except for a single analysis, not far from the edge (e, 13, -4.44‰). The nitrogen isotopic composition is much more variable (-3.5±1.4‰) and in particular it decreases to -7.5‰ at the rim. The nitrogen content, which is negatively correlated with $\delta^{15}N$ in ON-SLZ-390 and 391, also decreases initially in zone c where the $\delta^{15}N$ value is higher (spot 7), but in the inner and outer zones it correlates positively with $\delta^{15}N$, especially towards the rim (d-e, 10-13).

Discussion

The three cloudy diamonds we studied are unique within the group of superdeep diamonds due to their elevated N contents (Fig. 3a) and the presence of nano-inclusions of molecular nitrogen. Their carbon and nitrogen isotopic compositions fall within the respective mantle

ranges or expand to more positive $\delta^{15}N$ values, similar to other superdeep diamonds (Fig. 3b and 3c, Cartigny et al. 2014). Zones with low nitrogen content (<400 ppm) show a wide range of $\delta^{15}N$ (-7.5 to +0.87‰) while nitrogen-rich zones span a more restricted range ($\delta^{15}N$ of -2.9 to -7.1‰). The carbon isotopic composition of each diamond is highly uniform (except for the core of ON-SLZ-390), but as in the case of nitrogen, the largest deviations occur in the nitrogen-poor rim of ON-SLZ-392. Cartigny et al. (2014) have also noted higher variability of isotopic ratios in nitrogen poor zones.

Some of the observed variations can be explained by isotopic fractionation or the introduction of a new melt/fluid. For example, in ON-SLZ-390 the increase in the carbon isotopic ratios in the core (from -3.1 to -2.4‰,zones a and b in Fig. 1a) can be attributed to close system fractionation from an oxidized fluid (Petts et al. 2015) and the sharp change upon the transition from the core to zone c to introduction of a new fluid. In the CL image, this border is sharp and also represents a dissolution event, so it is logical to assume a change in the medium from which the diamond grew.

The concerted decrease in both $\delta^{15}N$ and [N] and the increase in $\delta^{13}C$ at the outer zones of diamond ON-SLZ-392 (Figure 2c) may also be the result of closed system fractionation, but from a fluid with a nitrogen speciation that produces different trends compared to the fractionation observed by Petts et al. (2015) where both $\delta^{15}N$ and $\delta^{13}C$ increased with the drop in nitrogen concentrations. Here, the carbon ratios increase, but the nitrogen ratios decreases towards the rim (Figure 2c). This type of nitrogen isotope fractionation, with a positive sign of the diamond-fluid fractionation factor, was previously described by Thomassot et al. (2007).

The case is different at the boundary between zone d and zone e in ON-SLZ-390. No dissolution took place on that boundary, and the CL image (Fig. 1a) only shows a change from oscillatory to homogenous growth without disruption. The carbon isotopic composition does not show any change on that boundary.

What scenario can be suggested to explain the large jump of the nitrogen content and isotopic composition between d and e in ON-SLZ-390? We could consider a third fluid that has exactly the same carbon isotopic ratio, but a much higher nitrogen concentration and a completely different nitrogen isotopic composition. Other explanations may rely on the higher sensitivity of nitrogen and its isotopes to changes in growth rates or to differences between different growth sectors or between planes of different orientation (e.g., cubic vs. octahedral).

The other two diamonds raise similar problems. The outer parts of ON-SLZ-391 are uniform except for two narrow bright bands (zones c and e) where [N] drops, $\delta^{15}N$ increases by more than 2‰ while carbon isotopes increase only by less than 0.2‰. ON-SLZ-392 shows a similar association of a bright CL band (zone c) with a sharp drop in [N] and a rise in $\delta^{15}N$ (at ~ constant $\delta^{13}C$). Such a spike was also observed by Petts et al. (2015, spot 33 in their profile). There too, a narrow band of very bright luminescence exhibits a strong spike in $\delta^{15}N$ (from -2.2‰ to +5.5‰ and back to -2.5‰) associated with a sharp drop in [N] (from 1400 to 300 and back to 1600 ppm). A second jump in $\delta^{15}N$ where luminescence is not bright (spot 19) is not accompanied by changes in [N] and $\delta^{13}C$.

Fractionation cannot produce the observed sharp variations. Introduction of a new fluid is possible, but it is hard to invoke a fluid that comes, deposits a thin layer of diamond and then disappears. Moreover, while the nitrogen content and nitrogen isotopic composition of this new fluid must be different, its carbon isotope ratio should be identical to that of the previous melt/fluid.

A change in the physico-chemical conditions, e.g., temperature, stress, redox conditions, pH, etc., may lead to changes in CL or nitrogen concentration of diamond (e.g. Babich et al. 2004). Such changes may affect the fractionation factors between the melt/fluid and the host diamond, or it may affect the fractionation through changes in the growth rate of diamond (Reutsky et al. 2017a). Again, it is hard to imagine such physico-chemical changes

that induce the observed variations and then dissipate without a trace, especially when the changes include strong variations in isotopic composition.

An alternative is that the observed sudden changes are not controlled by external factors, but by the diamond itself. The nitrogen isotope ratios in cubic growth sectors of synthetic diamonds are ~30‰ higher than in octahedral sectors (Boyd et al. 1988; Reutsky et al. 2008, 2017b). At the same time, the nitrogen content of the cubic sectors is much lower than that of the octahedral ones (Reutsky et al. 2017b). Is it possible that similar effects operate in natural diamonds? The effect was found to be much smaller in natural diamonds. Bulanova et al. (2002) studied a mixed-habit (cuboid and octahedral sectors present side by side) diamond and concluded that there was no fractionation of nitrogen isotopes between cubic and octahedral growth zones. However, re-examination of their data reveals a consistent average difference of ~1.2‰ in both C and N isotopic composition between simultaneously precipitated cuboid and octahedral growth layers (as shown by their CL image). The cuboid sectors are higher in $\delta^{13}C$ and $\delta^{15}N$ compared with the octahedral ones and are poorer in nitrogen. In both sectors, the isotope ratios increase during the growth of the diamond, but spots sampling contemporaneous growth in the two sectors are separated by about 1.2‰.

Howell et al. (2015) also noted minor fractionation between octahedral and cuboid growth sectors, but in the three "star" diamonds that they studied, they found no difference in the carbon isotopes and an average difference of 0.4-1‰ in $\delta^{15}N$ (with maximum differences between contemporaneous spots reaching 2‰). However, in this case the octahedral sector is richer in ^{15}N. Howell et al. (2015) also observed large differences in [N] between the two sectors. In the samples they studied, both sectors are rich in nitrogen but the octahedral sector (average ~2700 ppm) carries higher concentrations than the cuboid sector (~2000 ppm).

Fractionation between growth sectors potentially can provide an elegant explanation for the transition from zone c to zone d in ON-SLZ-390 and the fluctuations observed in

zones c and e of ON-SLZ-391 and zone c of ON-SLZ-392. Let us assume that these zones represent abrupt switches in the mode of growth (e.g., from octahedral to cuboid growth and back) and that these differences in growth direction lead to different incorporation of nitrogen and the favoring of ^{15}N over ^{14}N. In such a scenario, the diamonds could grow from a uniform melt or fluid, while the different surfaces incorporate different levels of nitrogen and different proportion of ^{15}N to ^{14}N. These inherently different layers behave differently during aggregation as well, leading to higher proportions of N3 centers and brighter CL.

This explanation may be more elegant than abrupt and very short lived mixing events, but it still is far from being completely satisfying . As discussed above, nitrogen isotopic fractionation between cuboid and octahedral growth sectors in natural diamonds is of the order of 2‰ or less. In addition, the bright-CL layers seem to be part of the concentric growth layers and not a sector of cubic growth. As such, the transition into the bright layers is different from the distinct sectors that grow in parallel in mixed-habit diamonds. They resemble, more closely, the transitions in cloudy and coated diamonds, or in samples where cuboid growth laminae are surrounded by octahedral surface and vice-versa (Lang 1974; Harte et al. 1999).

At this stage, we cannot conclude what the mechanism is that leads to the abrupt fluctuations in the isotopic composition and concentration of nitrogen in the growing diamond. It may reflect a change in the nature of the fluid. For example, a small batch of carbonatitic fluid that arrives, grows a thin layer and is reduced by the local environment. It may be a change in the physical conditions, e.g., a sudden rise or drop in temperature that changes the growth rate and leads to changes in the isotopic composition and the concentration of nitrogen. It can also be a sudden change in the growth directions, e.g., a switch from octahedral to cubic growth.

The fluctuations in nitrogen concentration and isotopic ratio between different zones must be attributed to the growth process. However, the luminescence in diamonds is the result

of color centers that may form not only during the growth process, but also later, as vacancies, interstitial carbon atoms, nitrogen atoms, and other minor impurities diffuse and react. The association between CL intensity and variations in the nitrogen concentration and isotopic composition shows that in addition to the growth process, post-formation reactions (e.g. aggregation) also proceed in a different manner in the different zones.

Conclusions

The three studied ultradeep diamonds from Sao Luiz, Brazil mostly exhibit uniform carbon isotopic compositions that fall within the known mantle range of -5±3‰ (Cartigny et al. 2014). Most of the nitrogen isotopic analyses also fall within the mantle range (-5±3‰). Some isotopic ratios we measured, associated with low nitrogen concentration and narrow zones of bright luminescence are higher, extending to positive $\delta^{15}N$ values. These sharp fluctuations cannot be attributed to fractionation in a fluid limited system and are not easily explained by short-lived introduction of a distinct diamond-forming melt or fluid. Alternative possibilities include sharp changes in the physical conditions during growth or fractionation between different growth directions (e.g., octahedral versus cuboid), so that contrasting nitrogen contents and isotopic compositions may form during diamond precipitation from a single melt/fluid. More gradual variations may be the result of Rayleigh fractionation or mixing. In the future, we need to combine in situ isotopic studies with nitrogen concentration and aggregation analyses on a similar scale, a better understanding of the CL record and documentation of the 3-D orientation of the growth-planes in order to achieve clearer insights into the growth of natural diamonds.

Acknowledgements. We thank DeBeers Consolidated mines for donating the samples. This publication stems from CCIM Project P1638. ON thanks grant # I-1239-301.8/2014 of the German–Israeli Foundation for Science and Development (GIF). TS acknowledges funding of the analytical costs through an NSERC Discovery Grant.

References

Babich YV, Feigelson BN, Yelisseyev AP (2004) Nitrogen aggregation and linear growth rate in HPHT synthetic diamonds. Diamond and Related Mmaterials, 13(10):1802-1806

Boyd SR, Pillinger CT, Milledge HJ, Mendelssohn MJ, Seal, M (1988) Fractionation of nitrogen isotopes in a synthetic diamond of mixed crystal habit. Nature, 331(6157):604-607

Bruley J, Brown LM (1989) Quantitative electron energy-loss spectroscopy microanalysis of platelet and voidite defects in natural diamond. Philosophical Magazine A, 59(2):247-261

Bulanova GP, Pearson DG, Hauri EH, Griffin BJ (2002). Carbon and nitrogen isotope systematics within a sector-growth diamond from the Mir kimberlite, Yakutia. Chemical Geology, 188(1):105-123

Bulanova GP, Walter MJ, Smith CB, Kohn SC, Armstrong LS, Blundy J, Gobbo L (2010) Mineral inclusions in sublithospheric diamonds from Collier 4 kimberlite pipe, Juina, Brazil: subducted protoliths, carbonated melts and primary kimberlite magmatism. Contributions to Mineralogy and Petrology 160(4):489-510

Cartigny P, Palot M, Thomassot E, Harris JW (2014) Diamond formation: a stable isotope perspective. Annual Review of Earth and Planetary Sciences, 42:699-732

Davies RM, Griffin WL, Pearson NJ, Andrew AS, Doyle BJ, O'Reilly SY (1999) Diamonds from the deep: pipe DO-27, Slave Craton, Canada. In: Gurney JJ, Gurney JL, Pascoe MD, Richardson SH,(Eds), The J.B. Dawson Volume, Proceedings of the VIIth International Kimberlite Conference, Red Roof Design, Capetown, 148–155.

Davies RM, Griffin WL, O'Reilly SY, McCandless TE (2004) Inclusions in diamonds from the K14 and K10 kimberlites, Buffalo Hills, Alberta, Canada: diamond growth in a plume? Lithos, 77(1):99-111

Davies RM, Griffin WL, O'Reilly SY, Doyle BJ (2004) Mineral inclusions and geochemical characteristics of microdiamonds from the DO27, A154, A21, A418, DO18, DD17 and Ranch Lake kimberlites at Lac de Gras, Slave Craton, Canada. Lithos, 77(1):39-55

Harte B, Fitzsimons ICW., Harris JW, Otter ML (1999) Carbon isotope ratios and nitrogen abundances in relation to cathodoluminescence characteristics for some diamonds from the Kaapvaal Province, S. Africa. Mineralogical Magazine, 63(6):829-829

Howell D, Stern RA, Griffin WL, Southworth R, Mikhail S, Stachel T (2015) Nitrogen isotope systematics and origins of mixed-habit diamonds. Geochimica et Cosmochimica Acta, 157:1-12

Hutchison MT, Cartigny P, Harris JW (1999) Carbon and nitrogen composition and physical characteristics of transition zone and lower mantle diamonds from Sa˜o Luiz, Brazil. In: Gurney JJ, Gurney JL, Pascoe MD, Richardson SH (eds) The J.B. Dawson Volume, Proceedings of the 7th International Kimberlite Conference. Red Roof Design, Capetown, pp 372–382

Javoy M, Pineau F, Delorme H (1986) Carbon and nitrogen isotopes in the mantle. Chemical geology, 57(1-2):41-62

Kagi H, Zedgenizov DA, Ohfuji H, Ishibashi H (2016) Micro- and nano-inclusions in a superdeep diamond from São Luiz, Brazil. Geochemistry International, 54(10):834-838

453 Kaminsky F, Zakharchenko O, Davies RM, Griffin WL, Khachatryan-Blinova G, Shiryaev A
454 (2001). Superdeep diamonds from the Juina area, Mato Grosso State, Brazil.
455 Contributions to Mineralogy and Petrology, 140(6):734-753
456 Kaminsky FV, Khachatryan GK, Andreazza P, Araujo D, Griffin WL (2009) Super-deep
457 diamonds from kimberlites in the Juina area, Mato Grosso State, Brazil. Lithos,
458 112:833-842
459 Kaminsky FV, Wirth R, Schreiber A (2015) A microinclusion of lower-mantle rock and other
460 mineral and nitrogen lower-mantle inclusions in a diamond. *The Canadian*
461 *Mineralogist*, 53(1):83-104
462 Kiflawi I, Bruley J (2000) The nitrogen aggregation sequence and the formation of voidites in
463 diamond. Diamond and related materials, 9(1):87-93
464 Lang AR (1974a) On the growthÿsectorial dependence of defects in natural diamonds.
465 Proceedings of the Royal Society of London, A340,233-248
466 Luyten W, van Tendeloo GV, Fallon PJ, Woods GS (1994) Electron microscopy and energy-
467 loss spectroscopy of voidites in pure type IaB diamonds. Philosophical Magazine A,
468 69(4):767-778.
469 Melton GL (2013) Elemental impurities, defects and carbon isotopes in mantle diamond
470 Doctoral dissertation, University of Alberta, Canada
471 Moore RO, Gurney JJ (1985) Pyroxene solid solution in garnets included in diamond. Nature,
472 318(6046):553-555
473 Navon O, Wirth R, Schmidt C, Jablon BM, Schreiber A, Emmanuel S (2017) Solid molecular
474 nitrogen (δ-N 2) inclusions in Juina diamonds: Exsolution at the base of the transition
475 zone. Earth and Planetary Science Letters. 464:237-47
476 Palot M, Pearson DG, Stern RA, Stachel T, Harris JW (2014) Isotopic constraints on the
477 nature and circulation of deep mantle C–H–O–N fluids: carbon and nitrogen

systematics within ultra-deep diamonds from Kankan (Guinea). Geochim. Cosmochim. Acta 139:26–46

Palot M, Pearson DG, Stachel T, Stern RA, Le Pioufle A, Gurney JJ, Harris JW (2017) The transition zone as a host for recycled volatiles: Evidence from nitrogen and carbon isotopes in ultra-deep diamonds from Monastery and Jagersfontein (South Africa). Chemical Geology, 466:733-749

Petts DC, Chacko T, Stachel T, Stern RA, Heaman LM (2015) A nitrogen isotope fractionation factor between diamond and its parental fluid derived from detailed SIMS analysis of a gem diamond and theoretical calculations. Chemical Geology, 410:188-200

Reutsky VN, Harte B, Borzdov YM, Palyanov YN (2008) Monitoring diamond crystal growth, a combined experimental and SIMS study. European Journal of Mineralogy, 20(3):365-374

Reutsky VN, Shiryaev AA, Titkov SV, Wiedenbeck M, Zudina NN (2017a) Evidence for large scale fractionation of carbon isotopes and of nitrogen impurity during crystallization of gem quality cubic diamonds from placers of North Yakutia. Geochem Int 55(11)

Reutsky VN, Kowalski PM, Palyanov YN, Wiedenbeck M (2017b) Experimental and theoretical evidence for surface-induced carbon and nitrogen fractionation during diamond crystallization at high temperatures and high pressures. Crystals 7(7):190, doi:10.3390/cryst7070190.

Rudloff-Grund J, Brenker FE, Marquardt K, Howell D, Schreiber A, O'Reilly SY, Griffin WL Kaminsky FV (2016) Nitrogen nanoinclusions in milky diamonds from Juina area, Mato Grosso State, Brazil. Lithos 265:57-67

Scott-Smith BS, Danchin RV, Harris JW, Stracke KJ (1984) Kimberlites near Orroroo, South Australia. In: Kimberlites I: kimberlites and related rocks, Elsevier, Amsterdam, 121-142

Stachel T, Harris J, Aulbach S, Deines P (2002) Kankan diamonds (Guinea) III: d 13 C and nitrogen characteristics of deep diamonds. Contributions to Mineralogy and Petrology, 142(4):465-475

Stern RA, Palot M, Howell D, Stachel T, Pearson DG, Cartigny P, Oh A (2014) Methods and Reference Materials for SIMS Diamond C- and N-isotope Analysis. Canadian Centre for Isotopic Microanalysis, Research Report 14-01 University of Alberta, Education and Research Archive http://hdl.handle.net/10402/era.38738.

Tappert R, Stachel T, Harris JW, Muehlenbachs K, Ludwig T, Brey GP (2005a) Diamonds from Jagersfontein (South Africa): messengers from the sublithospheric mantle. Contributions to Mineralogy and Petrology, 150(5):505-522

Tappert R, Stachel T, Harris JW, Muehlenbachs K, Ludwig T, Brey GP (2005b) Subducting oceanic crust: The source of deep diamonds. Geology, 33(7):565-568

Tappert R, Foden J, Stachel T, Muehlenbachs K, Tappert M, Wills K (2009) Deep mantle diamonds from South Australia: A record of Pacific subduction at the Gondwanan margin. Geology, 37(1):43-46

Taylor WR, Jaques AL, Ridd M (1990) Nitrogen-defect aggregation characteristics of some Australasian diamonds; time-temperature constraints on the source regions of pipe and alluvial diamonds. American Mineralogist 75(11-12):1290-1310

Taylor WR, Canil D Milledge J (1996) Kinetics of Ib to IaA nitrogen aggregation in diamond. Geochimica et Cosmochimica Acta, 60:4725-473

Wilding MC (1990) Untitled Ph.D. thesis: Edinburgh, University of Edinburgh, 281 pp

526 Woods GS (1986) Platelets and the Infrared-Absorption of Type-Ia Diamonds. Proceedings of
527 the Royal Society of London Series a-Mathematical Physical and Engineering
528 Sciences 407(1832):219-238
529 Zedgenizov DA, Kagi H, Shatsky VS, Ragozin AL (2014) Local variations of carbon isotope
530 composition in diamonds from São-Luis (Brazil): evidence for heterogenous carbon
531 reservoir in sublithospheric mantle. Chemical Geology 363:114-12.

Figure captions:

Fig. 1 CL of the three diamonds. The lines mark the measured profiles. The letters mark the zones of growth as described in the text. The tiny numbers along the yellow lines mark the analysis spots and can be seen in the online version

Fig. 2 $\delta^{13}C$, $\delta^{15}N$ and [N] along profiles from core to rim of the three diamonds. Upper panel: variation of $\delta^{13}C$ (blue diamonds), $\delta^{15}N$ (black squares) and [N] (red circles, secondary Y axis). Lower panel: a closer view at the correlation of $\delta^{13}C$ (primary axis, much finer scale) and $\delta^{15}N$ (secondary axis). No systematic correlation was observed. [N] and $\delta^{15}N$ exhibit negative correlations in ON-SLZ-391 and in the core of ON-SLZ-392, but decrease simultaneously towards the rim of ON-SLZ-392. Carbon and nitrogen isotopes vary together in ON-SLZ-391, but not in ON-SLZ-390 and 392. Letters below the panels denote the CL zones from Figure 1 for each analysis

Fig. 3 The relation between $\delta^{13}C$, $\delta^{15}N$ and [N] in the diamonds studied here compared with other diamonds from the transition zone and lower mantle. The three Sao Luiz samples are rich in nitrogen and have mantle-like $\delta^{13}C$ and $\delta^{15}N$ values. A few zones deviate to higher $\delta^{15}N$ values, similar to many lower mantle values. $\delta^{13}C$ values of transition zone diamonds and deep upper mantle diamonds extend to more negative values, down to -25‰ and to more positive $\delta^{15}N$ (Bulanova et al. 2010; Palot et al. 2017). Data sources: Wilding (1990), Hutchinson et al. (1999), Davies et al. (1999, 2004a, 2004b), Kaminsky et al. (2001, 2009), Stachel et al. (2002), Tappert et al. (2005a,b, 2009), Bulanova et al. (2010), Palot et al. (2012, 2017), Melton (2013), Zedgenizov et al. (2014)

Table 1. Carbon and nitrogen isotopic composition and nitrogen content

Zone[1]	Spot[a]	$\delta^{13}C$ (VPDB)[b]	2σ[c]	[N][d]	2σ	$\delta^{15}N$ (AIR)[e]	2σ	[N][f]
		‰	‰	ppm (Atomic)	ppm (Atomic)	‰	‰	ppm (Atomic)
ON-SLZ-390								
a	1	-3.12	0.13	4.6	0.3			
a	2	-2.90	0.13	3.8	0.2			
a	3	-2.55	0.13	2.5	0.2			
b	4	-2.42	0.15	0.7	0.1			
c	5	-3.26	0.14	182	6	-0.2	1.5	175
c	6	-3.16	0.14	5.9	0.4			
d	7	-3.26	0.12	164	5	+0.9	1.5	171
e	8	-3.24	0.17	996	31	-6.1	0.6	1043
e	9	-3.20	0.12	1041	39	-6.3	0.7	1112
e	10	-3.28	0.15	1014	37	-7.1	0.6	1098
e	11	-3.21	0.12	1049	36	-6.6	0.6	1094
e	12	-3.26	0.15	1075	34	-6.5	0.6	1105
e	13	-3.15	0.13	1019	33	-6.8	0.7	1063
e	14	-3.33	0.12	1064	34	-6.7	0.7	1069
e	15	-3.23	0.13	970	31	-7.0	0.6	1021
ON-SLZ-391								
a	1	-4.74	0.14	885	27	-3.1	0.7	977
a	2	-4.75	0.14	881	29	-3.2	0.7	931
a	3	-4.71	0.14	903	29	-3.1	0.6	1038
a	4	-4.73	0.15	663	22	-3.3	0.8	818
a	5	-4.75	0.14	816	28	-2.9	0.8	888
b	6	-4.86	0.15	1091	36	-4.0	0.7	1130
c	7	-4.71	0.14	338	11	+0.4	0.9	469
d	8	-4.83	0.13	1070	35	-3.5	0.6	1088
d	9	-4.74	0.12	1057	35	-3.7	0.6	1125
d	10	-4.87	0.16	1240	39	-4.0	0.6	1270
d	11	-4.79	0.14	1028	31	-4.0	0.6	1074
e	12	-4.57	0.14	338	10	-1.1	1.0	437
f	13	-4.75	0.14	1010	33	-4.5	0.6	1036
ON-SLZ-392								
a	1	-4.76	0.12	1198	37	-3.6	0.6	1224
a	2	-4.74	0.14	1176	40	-3.8	0.6	1196
a	3	-4.65	0.14	853	30	-5.4	0.7	880
b	4	-4.65	0.14	1212	41	-3.3	0.6	1240
b	5	-4.92	0.13	1230	41	-4.3	0.6	1246
b	6	-4.72	0.14	1105	35	-4.2	0.6	1133
c	7	-4.76	0.13	295	9	-1.6	1.2	286
d	8	-4.89	0.12	943	30	-4.7	0.7	954
b	9	-4.77	0.14	904	33	-0.6	0.7	945
b	10	-4.76	0.13	968	32	-3.7	0.7	1025
d	11	-4.88	0.12	837	26	-4.0	0.7	836
d	12	-4.67	0.16	521	16	-6.1	0.9	557
e	13	-4.44	0.12	191	6	-7.5	1.4	200
f	14	-4.81	0.13	32	1.2			

a. See Figure 1 for the definition of the zones and analysis spots.
b. Relative to the Vienna Pee Dee Belemnite with $^{13}C/^{12}C=0.01118$.
c. 2σ does not include error contributed by the reference materials.
d. Measured during the analysis of the carbon isotopic ratio.
e. Relative to air with $^{15}N/^{14}N=XXX$
f. Measured during the analysis of the nitrogen isotopic ratio on a spot adjacent to that of the carbon isotopic composition.

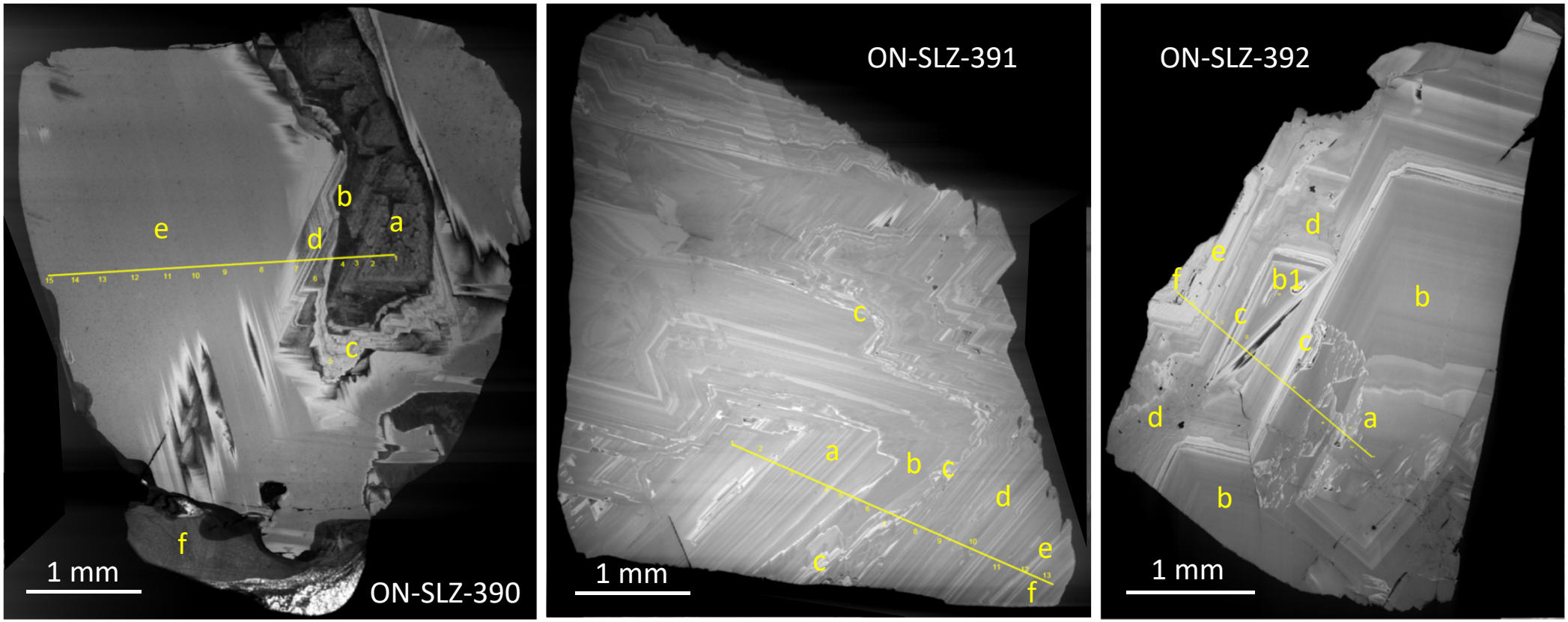

Fig. 1

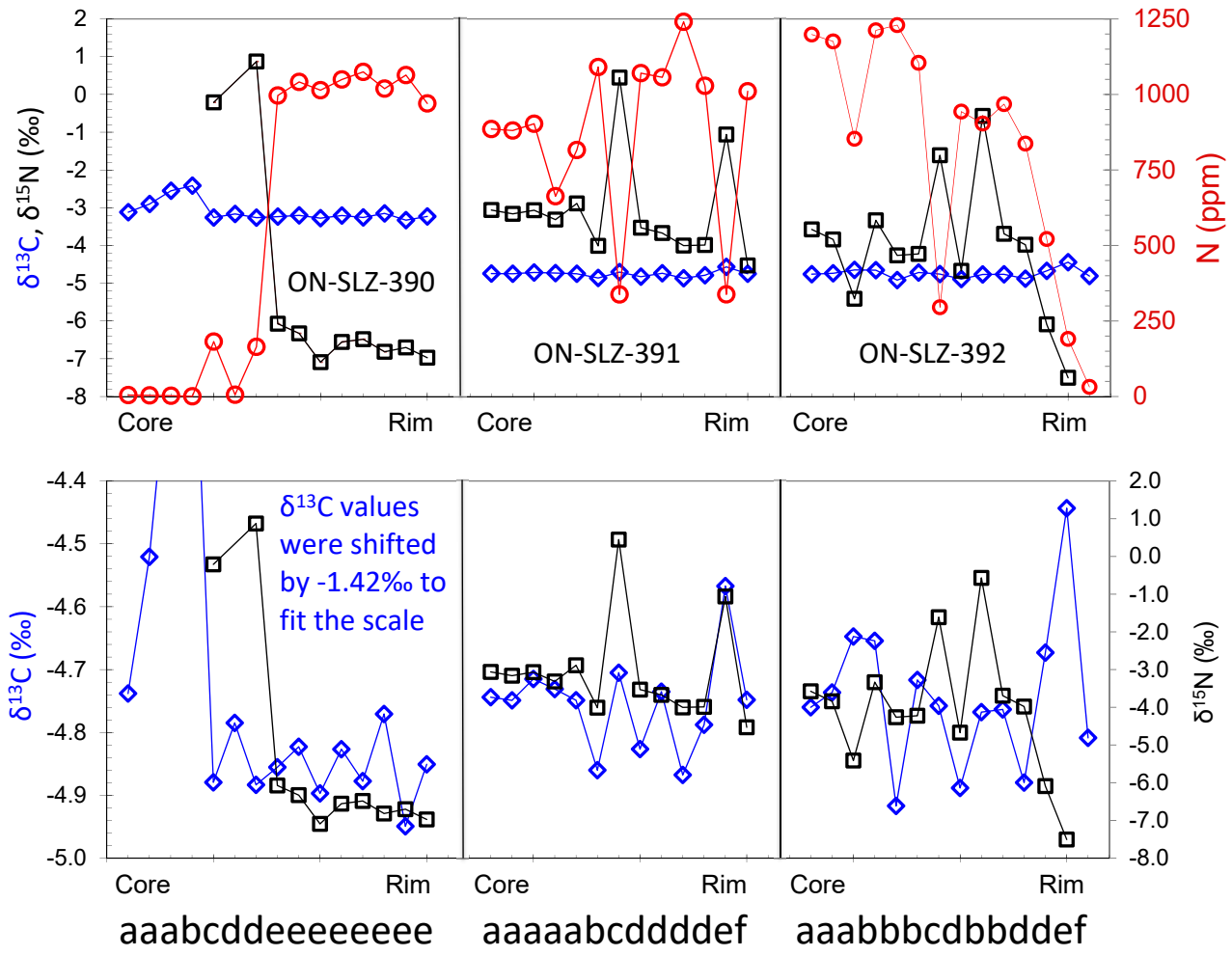

Fig. 2

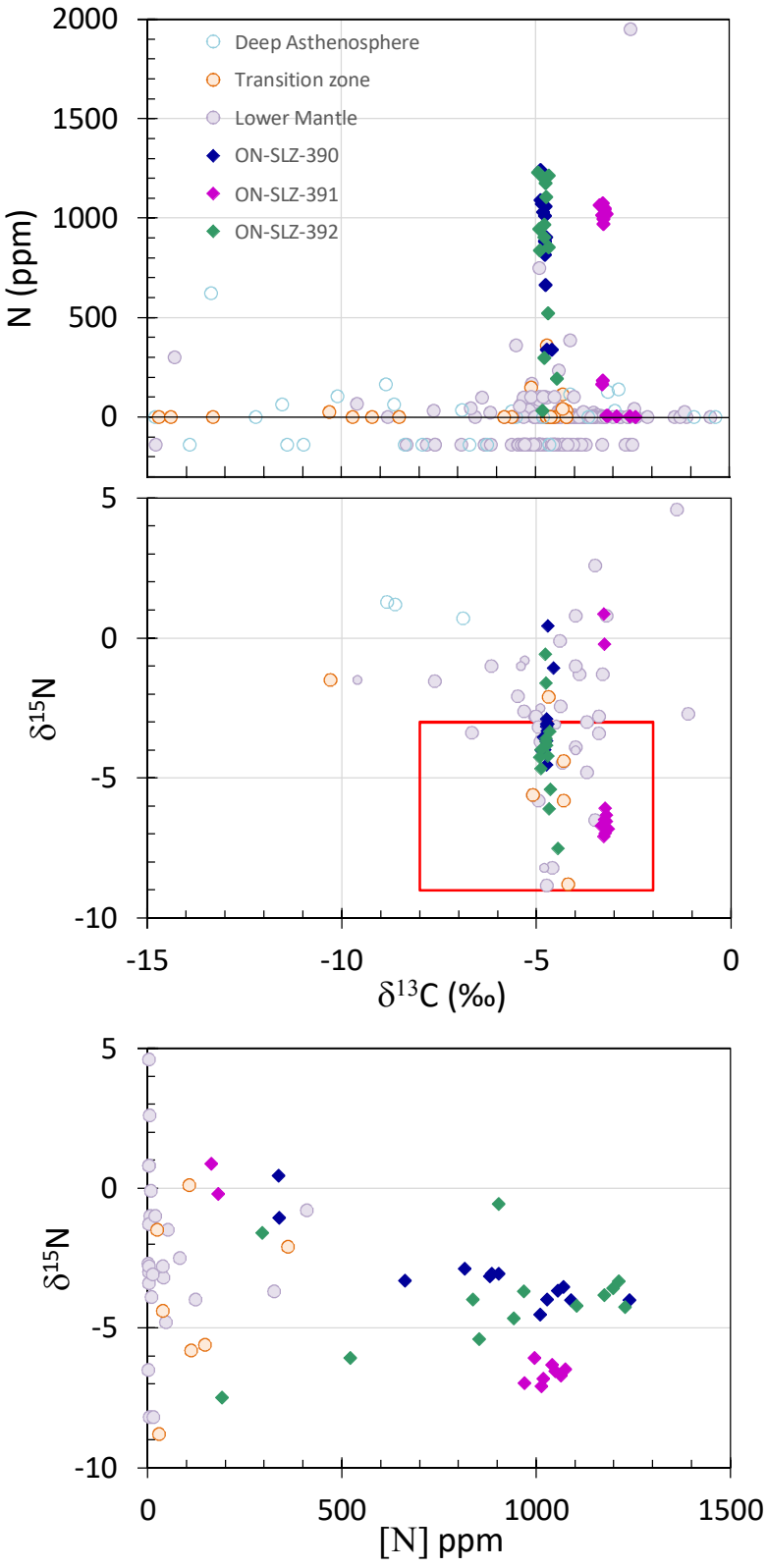

Fig. 3